Technical University of Denmark

DTU

Experimental and Modeling Investigation of the Effectof H2S Addition to Methane on the Ignition and Oxidation at High Pressures

Gersen, Sander; van Essen, Martijn; Darmeveil, Harry; Hashemi, Hamid; Rasmussen, Christian Tihic; Christensen, Jakob Munkholt; Glarborg, Peter; Levinsky, Howard

[Link back to DTU Orbit](#)

DTU Library
Technical Information Center of Denmark

Experimental and Modeling Investigation of the Effect of H$_2$S Addition to Methane on the Ignition and Oxidation at High Pressures

Sander Gersen,[†] Martijn van Essen,[†] Harry Darmeveil,[†] Hamid Hashemi,[‡] Christian Tihic Rasmussen,[‡] Jakob Munkholdt Christensen,[‡] Peter Glarborg,*[,‡] and Howard Levinsky[†,§]

[†]Oil & Gas, DNV GL, Post Office Box 2029, 9704 CA Groningen, Netherlands
[‡]DTU Chemical Engineering, Technical University of Denmark (DTU), 2800 Lyngby, Denmark
[§]Laboratory for High Temperature Energy Conversion Processes, University of Groningen, Nijenborgh 4, 9747 AG Groningen, Netherlands

Ⓢ *Supporting Information*

ABSTRACT: The autoignition and oxidation behavior of CH$_4$/H$_2$S mixtures has been studied experimentally in a rapid compression machine (RCM) and a high-pressure flow reactor. The RCM measurements show that the addition of 1% H$_2$S to methane reduces the autoignition delay time by a factor of 2 at pressures ranging from 30 to 80 bar and temperatures from 930 to 1050 K. The flow reactor experiments performed at 50 bar show that, for stoichiometric conditions, a large fraction of H$_2$S is already consumed at 600 K, while temperatures above 750 K are needed to oxidize 10% methane. A detailed chemical kinetic model has been established, describing the oxidation of CH$_4$ and H$_2$S as well as the formation and consumption of organosulfuric species. Computations with the model show good agreement with the ignition measurements, provided that reactions of H$_2$S and SH with peroxides (HO$_2$ and CH$_3$OO) are constrained. A comparison of the flow reactor data to modeling predictions shows satisfactory agreement under stoichiometric conditions, while at very reducing conditions, the model underestimates the consumption of both H$_2$S and CH$_4$. Similar to the RCM experiments, the presence of H$_2$S is predicted to promote oxidation of methane. Analysis of the calculations indicates a significant interaction between the oxidation chemistry of H$_2$S and CH$_4$, but this chemistry is not well understood at present. More work is desirable on the reactions of H$_2$S and SH with peroxides (HO$_2$ and CH$_3$OO) and the formation and consumption of organosulfuric compounds.

■ INTRODUCTION

The depletion of the traditional natural gas fields and the steadily increasing natural gas consumption have resulted in an increase in the global market share of gases from alternative sources. It is well-known that gases from these sources, such as shale gas, biogas, and so-called sour gas, may contain impurities that affect the combustion behavior of end-use equipment.[1] An important "impurity", present in, for example, sour gases, biogases, and some natural gases, is hydrogen sulfide (H$_2$S). The fraction of H$_2$S in sour gas can exceed several percent.[2]

The presence of trace amounts of H$_2$S can affect the combustion properties of fuels. Experimental results for fuel/H$_2$S interactions have been obtained in flow reactors, laminar premixed flames, and shock tubes. Selim et al. investigated the impact of H$_2$S on hydrogen[3,4] and methane[5,6] flames. Flow reactor studies of oxidation of CH$_4$/H$_2$S mixtures have been reported by Arutyunov et al.,[7] Chin et al.,[8] and Karan and Behie.[9] The flame and flow reactor studies are limited to a comparatively low pressure.

Of particular interest in the present work is the effect of H$_2$S on fuel ignition properties at elevated pressure. The impact of H$_2$S on H$_2$[10,11] and syngas[12] ignition delays has been investigated in shock tubes. Data obtained over a wide range of pressures (1.6−33 atm) and temperatures (1045−1860 K) show that low fractions of H$_2$S in H$_2$/O$_2$ mixtures increase the autoignition delay time, in some cases by a factor of 4 or more compared to neat H$_2$/O$_2$ mixtures.[11] In contrast with the

behavior of H$_2$/H$_2$S mixtures, modeling studies[13] indicate that the presence of H$_2$S reduces the autoignition delay times for methane at high pressures and intermediate temperatures, but no experimental data have been reported.

An improved understanding of the impact of small fractions of H$_2$S on the oxidation characteristics of hydrocarbon fuels is important for combustion equipment, such as homogeneous charge compression ignition (HCCI) engines, where auto-ignition is controlled for optimal performance. Furthermore, the occurrence of autoignition of the fuel/air mixture in spark-ignited gas engines leads to engine knock, which can reduce engine performance and cause engine damage. Understanding the effects of H$_2$S on the autoignition behavior of hydrocarbon fuels is thus essential for quantifying the impact of H$_2$S on the occurrence of knock in engines using natural gas. Moreover, experimental data, such as autoignition delay times and species profiles, are needed to develop and verify detailed chemical mechanisms.

In this paper, we present the results of experiments showing the effects of H$_2$S on methane ignition and oxidation. Autoignition measurements in a rapid compression machine

Table 1. Selected Reactions for the Hydrocarbon/Sulfur Interaction[a]

		A	β	E_a	source
R1	$SH + H_2O_2 \rightleftarrows H_2S + HO_2$	2.8×10^4	2.823	8668	11
R2	$SH + HO_2 \rightleftarrows H_2S + O_2$	3.8×10^4	2.775	−1529	19, 23
R3	$SH + HO_2 \rightleftarrows HSO + OH$	2.5×10^8	1.477	−2169	19, 23
R4	$SH + O_2 \rightleftarrows SO_2 + H$	1.5×10^5	2.123	11020	15
R5	$CH_3 + H_2S \rightleftharpoons CH_4 + SH$	6.8×10^7	1.200	1434	29
R6	$CH_3 + SH \rightleftharpoons CH_3SH$	7.3×10^{12}	0.230	−139	17
R7	$CH_3OO + SH \rightleftharpoons CH_3O + HSO$	2.5×10^7	1.477	−2169	b
R8	$CH_3OOH + SH \rightleftharpoons CH_3OO + H_2S$	5.6×10^3	2.823	8668	c
R9	$CH_3SH + H \rightleftharpoons CH_3S + H_2$	1.3×10^8	1.729	986	30
R10	$CH_3SH + H \rightleftharpoons CH_2SH + H_2$	4.1×10^3	2.925	4750	30
R11	$CH_3SH + H \rightleftharpoons CH_3 + H_2S$	7.1×10^{10}	0.766	3220	30
R12	$CH_3SH + H \rightleftharpoons CH_4 + SH$	7.0×10^6	1.983	16530	30
R13	$CH_3SH + O \rightleftharpoons CH_3S + OH$	4.2×10^7	1.818	80	31, d
R14	$CH_3SH + O \rightleftharpoons CH_2SH + OH$	3.3×10^3	2.864	1224	31, d
R15	$CH_3SH + OH \rightleftharpoons CH_3S + H_2O$	1.3×10^7	1.770	−1689	32
R16	$CH_3SH + OH \rightleftharpoons CH_2SH + H_2O$	1.9×10^5	2.220	718	32
R17	$CH_3SH + HO_2 \rightleftharpoons CH_3S + H_2O_2$	9.1×10^{12}	0.000	14300	33
R18	$CH_3SH + HO_2 \rightleftharpoons CH_2SH + H_2O_2$	2.0×10^{11}	0.000	14500	16
R19	$CH_3S + HO_2 \rightleftharpoons CH_3SH + O_2$	1.7×10^{-15}	7.490	−12060	34, e
R20	$CH_3SH + CH_3 \rightleftharpoons CH_3S + CH_4$	8.1×10^5	1.900	1700	16
R21	$CH_3SH + CH_3 \rightleftharpoons CH_2SH + CH_4$	1.5×10^{12}	0.000	6500	16
R22	$CH_3SH + SH \rightleftharpoons CH_3S + H_2S$	1.2×10^{14}	0.000	5920	17
R23	$CH_3S \rightleftharpoons CH_2S + H$	2.5×10^{38}	−7.800	62053	16
R24	$CH_3S + O_2 \rightleftharpoons CH_3 + SO_2$	9.5×10^{25}	−3.800	12300	35

[a]Parameters for use in the modified Arrhenius expression $k = AT^{\beta} \exp[-E/(RT)]$. Units are mol, cm, s, and cal. [b]Originally assumed the same as for $HO_2 + SH$,[23] but the A factor was reduced by a factor of 10 to comply with RCM measurements. [c]Originally assumed the same as for $H_2O_2 + SH$,[23] but the A factor was reduced by a factor of 10 to comply with RCM measurements. [d]Rate constant fitted in the present work to data reported. [e]From 200 to 800 K.

(RCM) at pressures ranging from 30 to 80 bar and temperatures from 930 to 1050 K are supplemented by measurements in a laminar flow reactor at 700−900 K and 50 bar. A detailed chemical kinetic model for ignition and oxidation of CH_4/H_2S mixtures is developed, starting from subsets for the oxidation of CH_4[14] and H_2S[15] as well as the formation and consumption of organosulfuric components.[16,17] Kinetic modeling of the experimental results provides insight into the chemistry of oxidation and serves to evaluate the predictive capability of the model.

DETAILED KINETIC MODEL

For this study, a chemical kinetic mechanism for the ignition of CH_4/H_2S mixtures has been constructed, with emphasis on reactions important at high pressure. The hydrocarbon subset of the mechanism was drawn from the recent work of Hashemi et al.,[14] who studied CH_4 oxidation and ignition at high pressure in a RCM and a flow reactor under conditions similar to those of the present study. This mechanism provides a good prediction of methane oxidation at high pressure over a wide range of conditions.

The H_2S subset was largely drawn from work of Haynes and co-workers. They investigated the chemistry of H_2S pyrolysis and oxidation in a series of modeling studies,[15,18,19] supported by ab initio calculations for key reactions.[20−25] The model of Zhou et al.,[19] which was developed to interpret atmospheric pressure flow reactor data, has formed the basis for more recent modeling work on H_2S oxidation[13,15,26] and impact of H_2S on H_2 ignition delays.[11] We have adopted the H_2S subset from the recent study of Song et al.,[15] who updated the mechanism of Zhou et al.[19] for application to high pressure.

The interaction between the hydrocarbon and sulfur subsets may involve the formation of methanethiol (CH_3SH) and subsequent conversion of organosulfuric species. Thermodynamic properties and rate constants in this subset were taken mostly from Zheng et al.[16] and van de Vijver et al.[17] Subsets for oxidation of CS_2 and OCS were drawn from previous work by the authors.[27,28] Selected reactions from the mechanism are listed in Table 1, and the key reactions are discussed in more detail below. The full mechanism is available in the Supporting Information.

Mathieu et al.[11] concluded that a better estimation of several rate constants was needed to improve predictions of H_2/H_2S ignition delays. Their predictions were particularly sensitive to the reaction of H_2S with HO_2 and the SH + SH reaction. The reaction of H_2S with HO_2

$$H_2S + HO_2 \rightleftharpoons SH + H_2O_2 \tag{R1b}$$
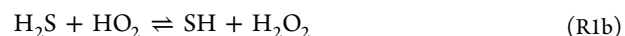
has been characterized experimentally at low temperature in both the forward[36] and reverse[37] directions, but only upper limit rate constants have been reported. Zhou[23] calculated the rate constant for the reverse step, $SH + H_2O_2 \rightleftharpoons H_2S + HO_2$ (reaction R1), from theory. Mathieu et al.[11] lowered the Zhou rate constant by a factor of 2 to improve agreement with their experiments. Recent calculations[33] indicate a much lower rate constant, but the level of theory (G3B3 and CBS-QB3) used was lower than that of Zhou.[23] In the present work, we have adopted the value of Mathieu et al.,[11] but an accurate determination of this rate constant is desirable.

Because the SH radical is comparatively unreactive toward O_2, its concentration builds up and modeling predictions may become sensitive to the SH + SH reaction. The two major

product channels for this reaction are $H_2S + S$, which initiates a chain-branching sequence ($S + O_2 \rightarrow SO + O$, and $SO + O_2 \rightarrow SO_2 + O$), and HSSH, which is terminating. We adopted the rate constant for $H_2S + S \rightleftharpoons SH + SH$ from Gao et al.,[38] while for the SH + SH recombination reaction, the high-pressure limit from Zhou et al.[25] was lowered by a factor of 4, following Song et al.[15]

In the recent modeling study of CH_4/H_2S oxidation by Bongartz and Ghoniem,[13] it was assumed that reactions of species containing both carbon and sulfur could be omitted from the reaction mechanism without a significant loss of accuracy. However, the present study indicates that direct interactions between hydrocarbon and sulfur species are important. This chemistry is quite complex. A number of relevant modeling studies have been reported recently in the literature on the pyrolysis of hydrocarbon/H_2S mixtures[39,40] as well as the pyrolysis[17] and oxidation[16] of hydrocarbon sulfides. Marin and co-workers[41−45] have conducted theoretical studies of the thermodynamics and kinetics of a range of organosulfur compounds, including various thiols and sulfides, and the mechanism of van de Vijver et al.[17] draws on this work.

In the present system, reactions of the CH_3 radical with the sulfur species pool include

$$CH_3 + H_2S \rightleftharpoons CH_4 + SH \tag{R5}$$

$$CH_3 + SH\,(+M) \rightleftharpoons CH_3SH\,(+M) \tag{R6}$$
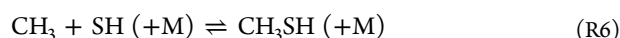
The reaction of CH_3 with H_2S has been studied experimentally at low to medium temperatures.[46,47] The theoretical studies by Mousavipour et al.[29] and very recently Zeng et al.[48] serve to extrapolate the experimental results to higher temperatures. For the recombination of CH_3 and SH to form CH_3SH (reaction R6), no measurements are available. An estimate of the second-order rate constant was drawn from the mechanism of van de Vijver et al.,[17] but an experimental or theoretical determination of the rate constant for reaction R6 over a range of pressures and temperatures is desirable.

At the conditions of the present experiments, with high pressure and low to intermediate temperatures, the peroxide chemistry is important for ignition and the interaction of peroxides with sulfur radicals may play a role. We have included in the model the two reactions.

$$CH_3OO + SH \rightleftharpoons CH_3O + HSO \tag{R7}$$

$$CH_3OOH + SH \rightleftharpoons CH_3OO + H_2S \tag{R8}$$
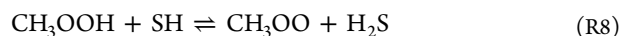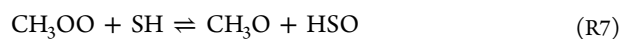
In the absence of experimental or theoretical data for the two steps, rate constants were initially estimated by analogy with the corresponding reactions of HO_2 and H_2O_2 with SH. However, as discussed below, reactions R7 and R8b strongly promote ignition and we had to reduce their rate constants by roughly an order of magnitude to avoid a severe underprediction of the ignition delays for CH_4/H_2S mixtures under RCM conditions.

The rate constants for the reactions of CH_3SH and its derived radicals (CH_3S and CH_2SH) were mostly taken from Zheng et al.[16] and van de Vijver et al.[17] Methanethiol is consumed by H-abstraction reactions to form mainly CH_3S (reactions R9, R13, R15, and R17), and the isomer CH_2SH is only formed in minor amounts (reactions R10, R14, R16, and R18).

The methylthiyl radical (CH_3S) may react with O_2 (reaction R24), the radical pool, or hydrocarbons and organosulfuric species to form larger molecules. For the $CH_3S + O_2$ reaction,

only room-temperature upper limits are available from the experiment.[49,50] It was studied theoretically by Zhu and Bozzelli.[35,51] At low temperatures, it forms a CH_3SOO adduct, but with a barrier to dissociation of only 10−11 kcal mol^{-1},[51,52] the adduct has a very limited thermal stability. At higher temperatures, the reaction proceeds to form SO_2.

$$CH_3S + O_2 \rightleftharpoons CH_3 + SO_2 \tag{R24}$$
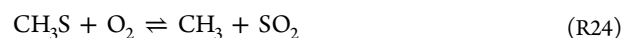
We have adopted the rate constant for reaction R24 calculated by Zhu and Bozzelli.[35]

Flow reactor studies for oxidation of CH_4/H_2S mixtures under reducing conditions show the formation of CS_2 and, to a smaller extent, OCS.[7,8] Presently, the conversion of the organosulfuric species to CS_2 and OCS is not well established, and this part of the mechanism needs to be revised.

■ EXPERIMENTAL SECTION

RCM. The autoignition measurements were performed in a RCM, which has been described in detail previously.[53,54] The compositions of the CH_4 and CH_4/H_2S (99:1) mixtures studied, expressed as mole percentages, are given in Table 2. The experiments were performed at

Table 2. Composition (Mole Fractions) of CH_4 and CH_4/H_2S (1% H_2S) Mixtures Used in the RCM Experiments Presented in Figures 2 and 3[a]

	number 1 (%)	number 2 (%)
CH_4	4.76	4.72
H_2S	0	0.052
O_2	19.05	19.05
N_2	30	30
Ar	46.19	46.18

[a]The fuel/air equivalence ratio was $\phi = 0.5$.

fuel-lean conditions (fuel/air equivalence ratios of $\phi = 0.5$), and the total concentration of diluting inert gases was close to that of nitrogen in air, while the Ar/N_2 ratio was chosen to provide temperatures (T_c) ranging from 930 to 1050 K and pressures (P_c) from 30 to 80 bar after compression. The gases used in the mixtures all have a purity greater than 99.99%. The pressure in the combustion chamber during compression and throughout the post-compression period was measured using a Kistler ThermoComp quartz pressure sensor with thermal-shock-optimized construction. A creviced piston head[55] was used to preserve a homogeneous reacting core gas during compression and during the post-compression period. The temperature after compression (T_c) is calculated on the basis of the known composition of the test mixtures, final pressure after compression (P_c), initial temperature and pressure, and assuming the existence of an adiabatic core.[55] The uncertainty of the calculated core gas temperature (T_c) is less than ±3.5 K for all measurements, and the day-to-day reproducibility of the measured autoignition delay time is within 10%.

The autoignition measurements in the RCM have been simulated using the homogeneous reactor software SENKIN[56] from the CHEMKIN library. To describe the compression and heat loss that occurred during the measurements, the specific volume of the assumed adiabatic core is used as input into the simulations. Because no multi-stage ignition phenomena were observed in the present work, we derive the specific volume directly from the measured pressure trace for the reactive mixture in the period between compression and the moment that substantial heat release begins using the isentropic relations of an ideal gas. Subsequently, we extrapolate the time dependence derived in this fashion to the region in which substantial heat release begins, as described in detail elsewhere.[53,54] Figure 1 shows an example of the measured and simulated pressure profiles.

Laminar Flow Reactor. A laboratory-scale high-pressure laminar flow reactor was used to study $CH_4/H_2S/O_2$ oxidation at 50 bar and
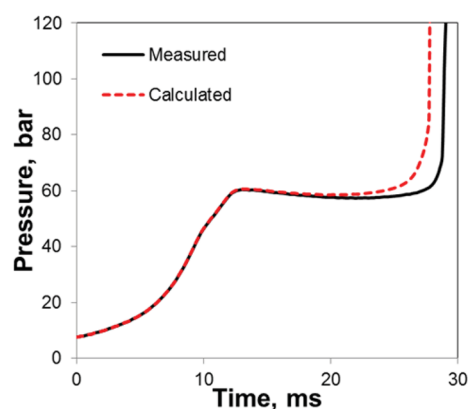
Figure 1. Measured (solid line) and simulated (dashed line) pressure profiles for mixture number 2 in Table 2 (99% CH_4 and 1% H_2S) at T_c = 927 K. The fuel/air equivalence ratio was ϕ = 0.5.

Figure 2. Measured (dots) and calculated (lines) autoignition delay times at a fixed pressure of P_c = 60 bar. The fuel/air equivalence ratio was ϕ = 0.5.

temperatures up to 900 K. The setup is described in detail elsewhere,[57] and only a brief description is provided here. The reactant gases were premixed before entering the reactor. The reactions took place in a tubular quartz reactor with an inner diameter of 8 mm and a total length of 154.5 cm. For the present operating conditions, the flow reactor was shown by Rasmussen et al.[57] to provide a good approximation to the plug flow. Using a quartz tube and conducting the experiments at high pressure, we expect the contribution from heterogeneous reactions at the reactor wall to be minimized. Our previous work on oxidation of neat CH_4 and H_2S[14,15] showed no indications of surface effects. The temperature profile in the flow reactor was measured inside the quartz tube. The residence time in the isothermal zone of the reactor was 6.6−10.0 s with the current flow rate of 3.0 NL/min (273 K and 1 atm) and temperatures in the range of 600−900 K. The adiabatic temperature rise as a result of the heat of reaction at full oxidation was calculated to be 22 K. However, as a result of the limited conversion and heat transfer from the hot gas to the surroundings, the actual temperature rise would be considerably lower. All gases used in the experiments were high-purity gases or mixtures with certified concentrations (±2% uncertainty). The product analysis was conducted at the outlet of the reactor by an online 6890N Agilent gas chromatograph (GC−TCD/FID from Agilent Technologies). The relative measuring uncertainty of the GC was in the range of ±6%.

RESULTS AND DISCUSSION

Autoignition Delay Times in the RCM. Figure 2 presents the autoignition delay times measured as a function of the temperature T_c at a fixed pressure of $P_c \sim$ 60 bar, and in Figure 3, measurements are presented at a fixed temperature of $T_c \sim$ 970 ± 3.5 K for pressures ranging from $P_c \sim$ 30 to 80 bar (see Table 2 for the compositions used). The results show that the addition of 1% H_2S to methane decreases the autoignition delay time by about a factor of 2 for all temperatures and pressures measured. The promoting effect of H_2S on oxidation is in agreement with the flow reactor results described below. In contrast, the addition of low fractions of H_2S to hydrogen[11] was seen to result in a substantial increase in the autoignition delay time at pressures around 33 bar and temperatures higher than 1190 K, while at lower temperatures, H_2S addition to hydrogen was seen to reduce the delay time only slightly compared to pure H_2.

Figures 2 and 3 compare the autoignition measurements to the predicted ignition delay times. The calculated and observed autoignition delay times for pure CH_4 and the CH_4/H_2S mixtures are in good agreement for the measured pressures and temperatures.
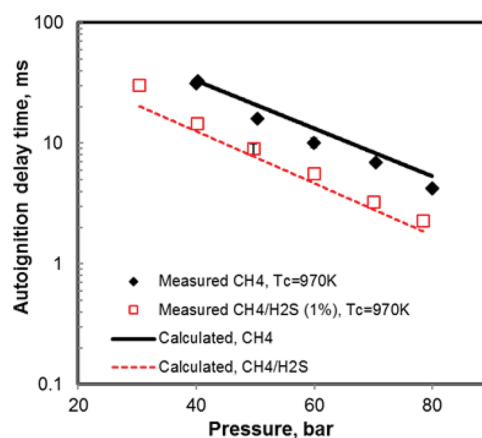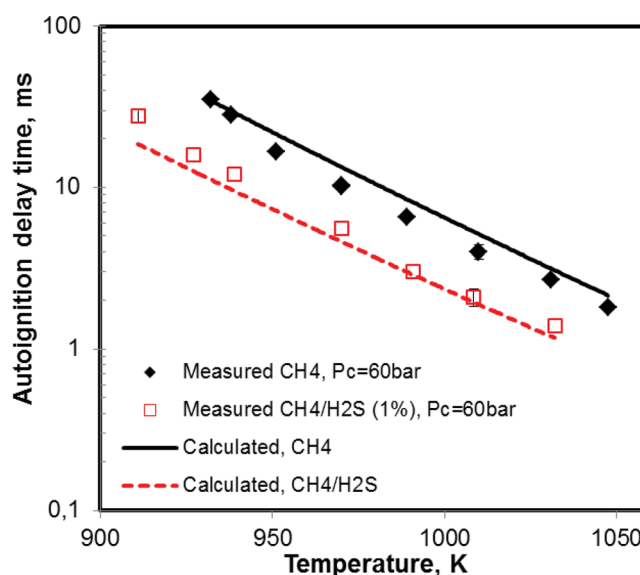

Figure 3. Measured (dots) and calculated (lines) autoignition delay times at a fixed temperature of T_c = 970 K. The fuel/air equivalence ratio was ϕ = 0.5.

To analyze the effect of H_2S on ignition under these experimental conditions, reaction path and sensitivity analyses were conducted. The results shown in Figures 4 and 5 have been performed for 80 bar and 970 K. The sensitivity coefficients are obtained using

$$S_{T,i} = \frac{(\Delta\tau/\tau)}{(\Delta k_i/k_i)} \qquad (1)$$

A positive sensitivity coefficient S_T indicates that an increase in the reaction rate constant leads to an increase in the predicted autoignition delay time. The sensitivity analysis shows that the predicted autoignition delay time is strongly sensitive to the reaction of methane with the radicals OH and HO_2

$$CH_4 + OH \rightleftharpoons CH_3 + H_2O$$

$$CH_4 + HO_2 \rightleftharpoons CH_3 + H_2O_2$$
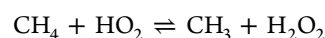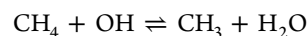
and to the fate of the relatively unreactive methyl radicals. At the high pressure, the peroxide chemistry becomes important for the predicted ignition delay as discussed in detail by
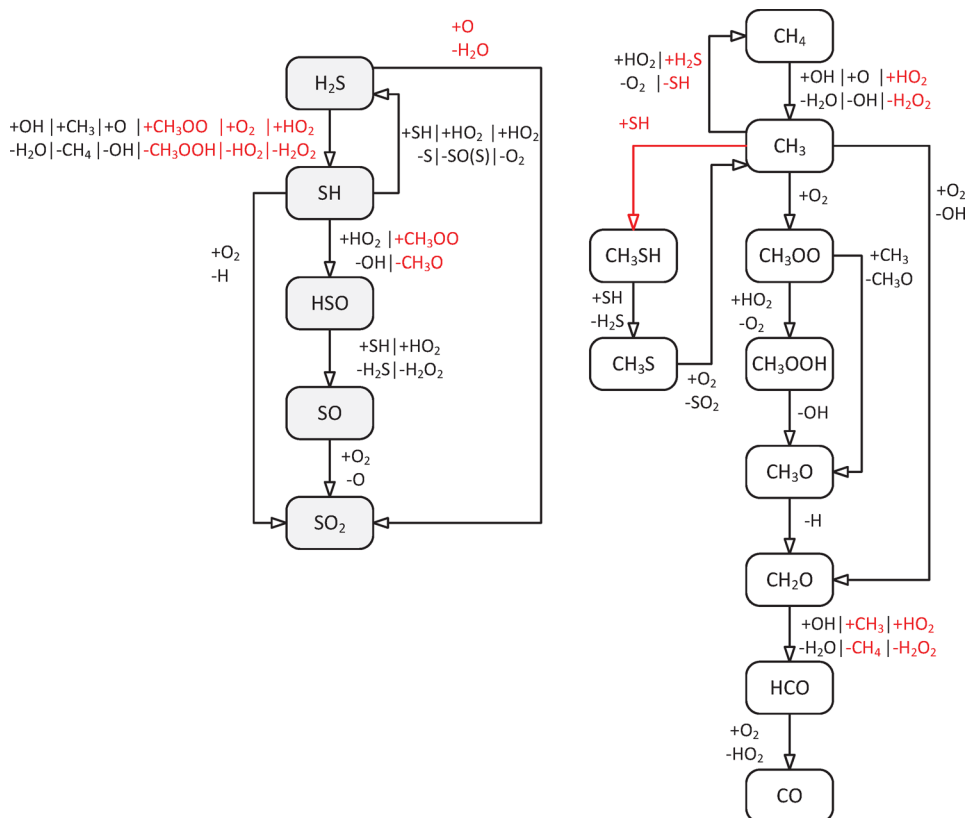
Figure 4. Reaction pathways for CH_4 and H_2S oxidation under RCM (970 K and 80 bar) and flow reactor conditions (800 K and 50 bar). The reactions colored red are involved only under RCM conditions. Only the C1 pathway is shown for CH_4.
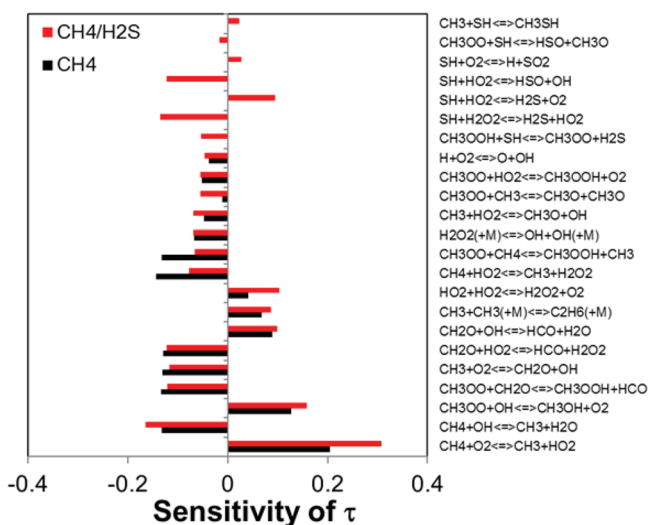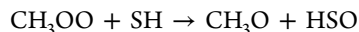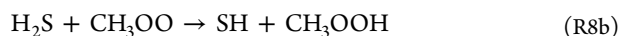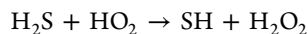

Figure 5. Sensitivity coefficients with respect to the autoignition delay time calculated at $T_c = 970$ K and $P_c = 80$ bar at fuel-lean conditions ($\phi = 0.5$) for CH_4 (black bars) and CH_4/H_2S (red bars) with 1% H_2S.

Hashemi et al.[14] The formation of HO_2 and H_2O_2 as well as CH_3OO and CH_3OOH plays an important role in the oxidation of both methane and the methyl radical. The methyl radical is converted to CH_2O directly by reaction with O_2 and indirectly via $CH_3 \xrightarrow{+HO_2} CH_3O \xrightarrow{+M,O_2} CH_2O$, $CH_3 \xrightarrow{+O_2} CH_3OO \xrightarrow{+HO_2,CH_4,CH_2O} CH_3OOH \xrightarrow{+M} CH_3O \xrightarrow{+M,O_2} CH_2O$, and $CH_3 \xrightarrow{+O_2} CH_3OO \xrightarrow{+CH_3} CH_3O \xrightarrow{+M,O_2} CH_2O$. Hydrogen peroxide, formed from H-abstraction reactions of HO_2, yields

OH radicals via thermal dissociation, H_2O_2 (+M) → OH + OH (+M), further promoting oxidation of methane.

When H_2S is added to methane, reactions between H_2S and peroxides and between methyl peroxide and SH become competitive with reactions in the methane oxidation subset and serve to promote ignition.

$$H_2S + HO_2 \rightarrow SH + H_2O_2$$

$$H_2S + CH_3OO \rightarrow SH + CH_3OOH \quad (R8b)$$

$$CH_3OO + SH \rightarrow CH_3O + HSO$$

The modeling predictions appear to support the value of k_1 proposed by Mathieu et al.,[11] but rate constants for several of the key sulfur reactions are uncertain. To obtain an acceptable agreement between predictions and experiment, we found it necessary to decrease the rate constants for reactions R7 and R8 by an order of magnitude compared to the values calculated by Zhou[23] for the similar reactions of HO_2.

The reaction path and sensitivity analyses presented in Figures 4 and 5 indicate that the addition of H_2S to methane has an impact on both the O/H radical pool and the hydrocarbon oxidation channels. The interaction between H_2S and the H_2/O_2 subset plays an important role in the formation of chain carriers in the early stage of the ignition process. The rapid formation of OH radicals in the early stage, mainly through the sequence $H_2S + HO_2 \rightarrow SH + H_2O_2$ (reaction R1b), H_2O_2 (+M) → OH + OH (+M), SH + HO_2 = HSO + OH (reaction R3), enhances the ignition process. Ignition is further promoted by reaction of H_2S (reaction R8b) and SH (reaction R7) with the CH_3OO radical, while recombination of CH_3 and SH (reaction R6), feeding into

the organosulfuric species pool, and $SH + HO_2 \rightarrow H_2S + O_2$ (reaction R2) are chain-terminating.

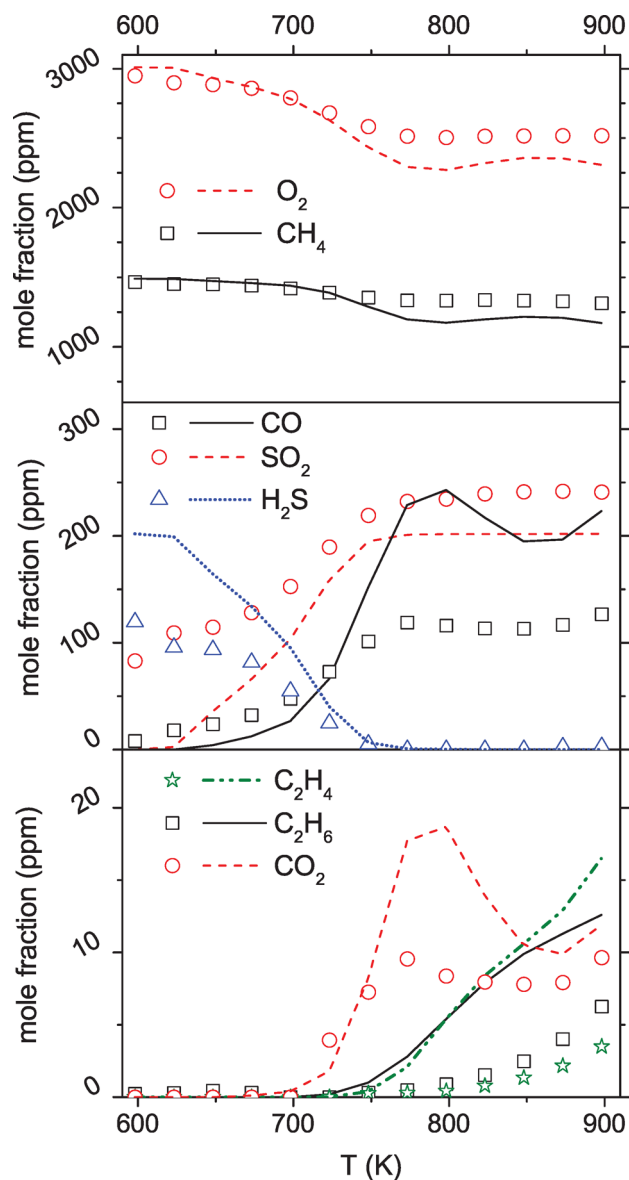**Oxidation in the Flow Reactor.** The flow reactor experiments were conducted at 50 bar and fuel/air equivalence ratios of $\phi = 22.8$ ($H_2S/CH_4 \sim 1.6\%$) and $\phi = 1.1$ ($H_2S/CH_4 \sim 14\%$). Figures 6 and 7 compare measured and predicted
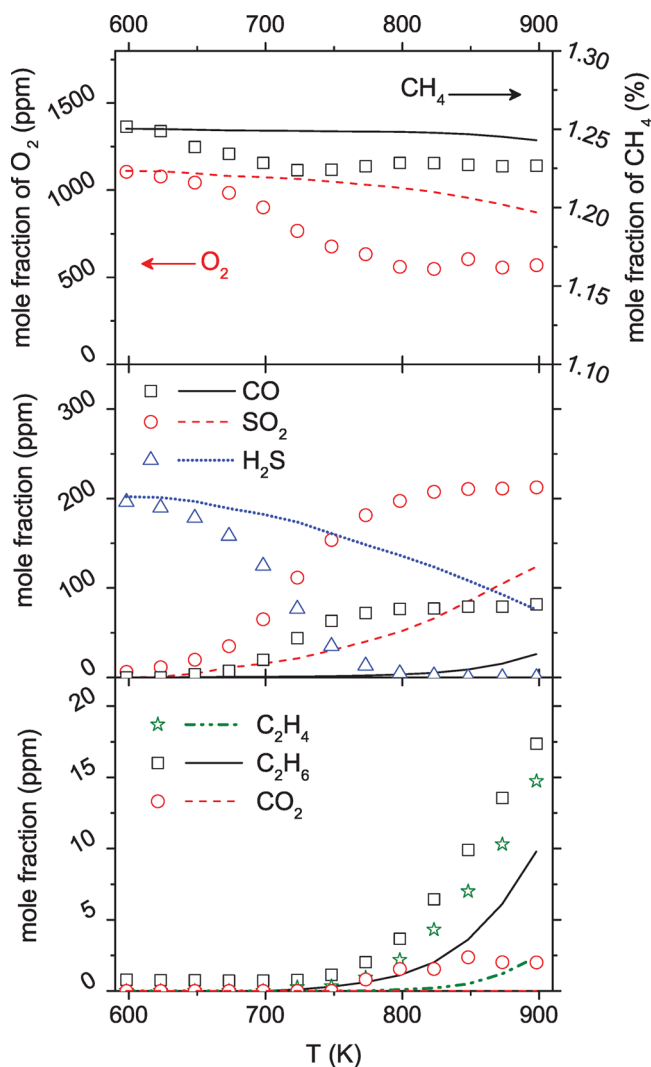
Figure 6. Results of experiments with CH_4/H_2S in the flow reactor at 50 bar. Inlet composition: 1.25% CH_4, 1110 ppm of O_2, 200 ppm of H_2S, and balance N_2 ($\phi = 22.8$). The gas residence time is calculated as τ (s) = 5990/T (K).

Figure 7. Results of experiments with CH_4/H_2S in the flow reactor at 50 bar. Inlet composition: 1500 ppm of CH_4, 3010 ppm of O_2, 200 ppm of H_2S, and balance N_2 ($\phi = 1.1$). The gas residence time is calculated as τ (s) = 5920/T (K).

species fractions in the outlet of the reactor versus the reactor temperature. For the fuel-rich mixture, the onset of H_2S oxidation (10% conversion) is around 650 K. At this temperature, roughly 6% oxygen is consumed and the major product is SO_2. Above 750 K, H_2S is completely consumed. Sulfur dioxide remains the major product, even at higher temperatures, because methane conversion is very limited under these conditions.

For the stoichiometric mixture, about 40% H_2S has been consumed already at 600 K, where CH_4 is largely unreacted. A 10% conversion of oxygen is achieved at 725 K, while a temperature of 775 K is needed to oxidize 10% methane. Similar to fuel-rich conditions, the methane conversion is limited; therefore, the major product is SO_2. The sulfur and

carbon balances close within 8 and 2%, respectively, throughout the experiments. For the fuel-rich case, however, a considerable amount of oxygen (up to 28%) is not taken into account; presumably this difference is due to formation of unmeasured oxygenated products.

Under very fuel-rich conditions (Figure 6), the model severely underpredicts the observed conversion of both H_2S and CH_4. Under stoichiometric conditions (Figure 7), predictions are in better agreement with the measurements. The major difference is that the model predicts the onset of H_2S conversion to occur at 700 K, while the experimental data indicate H_2S oxidation even below 600 K. The onset of the reaction for CH_4 and O_2 at around 725 K is captured well by the model, while above 750 K, the consumption of these reactants is slightly overpredicted, resulting in overprediction of the concentrations of C_2H_4, CO, and CO_2. Comparisons to simulations for undoped mixtures of CH_4/O_2 (data not shown) indicate a promoting effect of H_2S on methane oxidation,

similar to what was observed in the RCM experiments. The predicted methane conversion is negligible at temperatures below 850 K for neat mixtures of CH_4/O_2 (both stoichiometries), while for mixtures of $CH_4/O_2/H_2S$, the temperature for the onset of the reaction is calculated to be about 700 K.

As shown in the reaction pathway diagram for CH_4/H_2S oxidation (Figure 4), oxidation pathways for the flow reactor conditions are similar to those predicted for the RCM. However, the results must be interpreted cautiously as a result of the discrepancies between modeling predictions and experimental data. Figure 8 shows the sensitivity of the model predictions toward reaction rate constants for both stoichiometries at 725 K.

According to the model, the reaction $H_2S + O_2 = SH + HO_2$ initiates the H_2S oxidation. The fate of the SH radical is important for the oxidation of both CH_4 and H_2S. Predictions are particularly sensitive to the branching fraction of the SH + HO_2 reaction between HSO + OH (reaction R3, chain
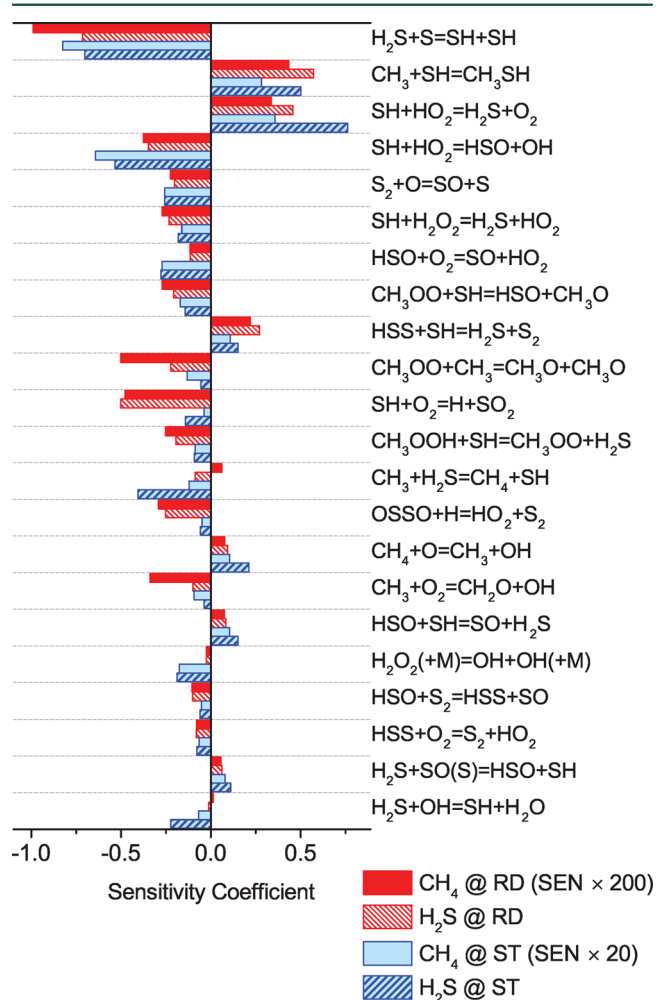
Figure 8. Sensitivity of reaction rate constants in predicting H_2S and CH_4 mole concentrations at 25% conversion of H_2S [time = 11.4 s (RD) and 1.2 s (ST)] at 800 K and 50 bar. RD, reducing (fuel-rich) conditions; ST, stoichiometric conditions. Other conditions are similar to those in the captions of Figures 6 and 7. The sensitivity coefficients are calculated as $S = -((X_{H_2S} - X_{H_2S,0})/X_{H_2S,0})/((k - k_0)/k_0)$, where k and X represent the rate constant and molar fraction, respectively. Only the 10 most sensitive reactions for each case are shown.

propagating) and $H_2S + O_2$ (reaction R2, terminating). Also the reactions $SH + O_2 \rightarrow SO_2 + H$ (reaction R4) and $SH + SH \rightarrow H_2S + S$ promote oxidation, while recombination of SH with CH_3 (reaction R6) inhibits reaction. In line with findings for high-pressure oxidation of neat methane,[14] reactions involving the CH_3OO radical are rate-controlling for the CH_4/H_2S mixture. Similar to the RCM conditions, reactions of H_2S (reaction R8b) and SH (reaction R7) with the CH_3OO radical strongly promote oxidation.

SUMMARY AND CONCLUSION

The autoignition and oxidation behavior of CH_4/H_2S mixtures have been studied experimentally in a RCM and flow reactor. The results were interpreted in terms of a detailed chemical kinetic model, describing the oxidation of CH_4 and H_2S as well as the formation and consumption of organosulfuric species. Autoignition measurements performed in a RCM at pressures of 30−80 bar and temperatures from 930 to 1050 K show that the addition of 1% H_2S to methane reduces the autoignition delay time by a factor of 2 compared to neat methane. Predictions with the model agree well with the measured autoignition delay times, provided that reactions of H_2S and SH with peroxides (HO_2 and CH_3OO) are constrained.

In the flow reactor at 50 bar and temperatures of 600−900 K, a large part of H_2S is consumed already at 600 K. while temperatures around 775 K are needed to oxidize 10% methane. Similar to the RCM results, H_2S has a promoting effect on the oxidation of methane. A comparison of the flow reactor data to modeling predictions shows satisfactory agreement under stoichiometric conditions, while at very reducing conditions, the model underestimates the consumption of both H_2S and CH_4. Our work indicates that the H_2S oxidation chemistry and the interaction of CH_4 and H_2S at high pressure are not well understood. More work is desirable on the reactions of H_2S and SH with peroxides (HO_2 and CH_3OO) and the formation and consumption of organosulfuric compounds.

ASSOCIATED CONTENT

Ⓢ Supporting Information

The Supporting Information is available free of charge on the ACS Publications website at DOI: 10.1021/acs.energy-fuels.6b02140.

Full mechanism (TXT)
Thermodynamic properties (TXT)

AUTHOR INFORMATION

Corresponding Author
*E-mail: pgl@kt.dtu.dk.

ORCID Ⓘ
Hamid Hashemi: 0000-0002-1002-0430
Peter Glarborg: 0000-0002-6856-852X

Notes
The authors declare no competing financial interest.

ACKNOWLEDGMENTS

■ REFERENCES

(1) Turkin, A. A.; Dutka, M.; Vainchtein, D.; Gersen, S.; van Essen, V. M.; Visser, P.; Mokhov, A. V.; Levinsky, H. B.; De Hosson, J. Th. M. *Appl. Energy* **2014**, *113*, 1141−1148.

(2) Schobert, H. H. *The Chemistry of Hydrocarbon Fuels*; Butterworth & Co.: London, U.K., 1990.

(3) Selim, H.; Ibrahim, S.; Al Shoaibi, A.; Gupta, A. K. *Appl. Energy* **2013**, *109*, 119−124.

(4) Selim, H.; Ibrahim, S.; Al Shoaibi, A.; Gupta, A. K. *Appl. Energy* **2014**, *113*, 1134−1140.

(5) Selim, H.; Al Shoaibi, A.; Gupta, A. K. *Appl. Energy* **2011**, *88*, 2593−2600.

(6) Selim, H.; Al Shoaibi, A.; Gupta, A. K. *Appl. Energy* **2012**, *92*, 57−64.

(7) Arutyunov, V. S.; Vedeneev, V. L.; Nikisha, L. V.; Polyak, S. S.; Romanovich, L. B.; Sokolov, O. V. *Kinet. Catal.* **1993**, *34*, 223−226.

(8) Chin, H. S. F.; Karan, K.; Mehrotra, A. K.; Behie, L. A. *Can. J. Chem. Eng.* **2001**, *79*, 482−490.

(9) Karan, K.; Behie, L. A. *Ind. Eng. Chem. Res.* **2004**, *43*, 3304−3313.

(10) Bradley, J. N.; Dobson, D. C. *J. Chem. Phys.* **1967**, *46*, 2872−2875.

(11) Mathieu, O.; Deguillaume, F.; Petersen, E. L. *Combust. Flame* **2014**, *161*, 23−36.

(12) Mathieu, O.; Hargis, J.; Camou, A.; Mulvihill, C.; Petersen, E. L. *Proc. Combust. Inst.* **2015**, *35*, 3143−3150.

(13) Bongartz, D.; Ghoniem, A. F. *Combust. Flame* **2015**, *162*, 2749−2757.

(14) Hashemi, H.; Christensen, J. M.; Gersen, S.; Levinsky, H. B.; Klippenstein, S. J.; Glarborg, P. *Combust. Flame* **2016**, *172*, 349−364.

(15) Song, Y.; Hashemi, H.; Christensen, J. M.; Zou, C.; Haynes, B.; Marshall, P.; Glarborg, P. *Int. J. Chem. Kinet.* **2016**, DOI: 10.1002/kin.21055.

(16) Zheng, X.; Bozzelli, J. W.; Fisher, E. M.; Gouldin, F. C.; Zhu, L. *Proc. Combust. Inst.* **2011**, *33*, 467−475.

(17) Van de Vijver, R.; Vandewiele, N. M.; Vandeputte, A. G.; Van Geem, K. M.; Reyniers, M.-F.; Green, W. H.; Marin, G. B. *Chem. Eng. J.* **2015**, *278*, 385−393.

(18) Sendt, K.; Jazbec, M.; Haynes, B. S. *Proc. Combust. Inst.* **2002**, *29*, 2439−2446.

(19) Zhou, C.; Sendt, K.; Haynes, B. S. *Proc. Combust. Inst.* **2013**, *34*, 625−632.

(20) Montoya, A.; Sendt, K.; Haynes, B. S. *J. Phys. Chem. A* **2005**, *109*, 1057−1062.

(21) Sendt, K.; Haynes, B. S. *J. Phys. Chem. A* **2005**, *109*, 8180−8186.

(22) Sendt, K.; Haynes, B. S. *Proc. Combust. Inst.* **2007**, *31*, 257−265.

(23) Zhou, C. Kinetic study of the oxidation of hydrogen sulfide. Ph.D. Thesis, The University of Sydney, Sydney, New South Wales, Australia, 2009.

(24) Zhou, C.; Sendt, K.; Haynes, B. S. *J. Phys. Chem. A* **2009**, *113*, 2975−2981.

(25) Zhou, C.; Sendt, K.; Haynes, B. S. *J. Phys. Chem. A* **2009**, *113*, 8299−8306.

(26) Bongartz, D.; Ghoniem, A. F. *Combust. Flame* **2015**, *162*, 544−553.

(27) Glarborg, P.; Marshall, P. *Int. J. Chem. Kinet.* **2013**, *45*, 429−439.

(28) Glarborg, P.; Halaburt, B.; Marshall, P.; Guillory, A.; Troe, J.; Thellefsen, M.; Christensen, K. *J. Phys. Chem. A* **2014**, *118*, 6798−6809.

(29) Mousavipour, S. H.; Namdar-Ghanbari, M. A.; Sadeghian, L. *J. Phys. Chem. A* **2003**, *107*, 3752−3758.

(30) Kerr, K. E.; Alecu, I. M.; Thompson, K. M.; Gao, Y.; Marshall, P. *J. Phys. Chem. A* **2015**, *119*, 7352−7360.

(31) Cardoso, D. V. V.; de Araújo Ferrão, L. F.; Spada, R. F. K.; Roberto-Neto, O.; Machado, F. B. C. *Int. J. Quantum Chem.* **2012**, *112*, 3269−3275.

(32) Masgrau, L.; Gonzalez-Lafont, A.; Lluch, J. M. *J. Phys. Chem. A* **2003**, *107*, 4490−4496.

(33) Batiha, M.; Altarawneh, M.; Al-Harahsheh, M.; Altarawneh, I.; Rawadieh, S. *Comput. Theor. Chem.* **2011**, *970*, 1−5.

(34) Liu, Y.; Wang, W.; Zhang, T.; Cao, J.; Wang, W.; Zhang, Y. *Comput. Theor. Chem.* **2011**, *964*, 169−175.

(35) Zhu, L.; Bozzelli, J. W. *J. Phys. Chem. A* **2006**, *110*, 6923−6937.

(36) Mellouki, A.; Ravishankara, A. R. *Int. J. Chem. Kinet.* **1994**, *26*, 355−365.

(37) Friedl, R. R.; Brune, W. H.; Anderson, J. G. *J. Phys. Chem.* **1985**, *89*, 5505−5510.

(38) Gao, Y.; Zhou, C.; Sendt, K.; Haynes, B. S.; Marshall, P. *Proc. Combust. Inst.* **2011**, *33*, 459−465.

(39) Nguyen, V. P.; Burkle-Vitzthum, V.; Marquaire, P. M.; Michels, R. *J. Anal. Appl. Pyrolysis* **2013**, *103*, 307−319.

(40) Nguyen, V. P.; Burkle-Vitzthum, V.; Marquaire, P. M.; Michels, R. *J. Anal. Appl. Pyrolysis* **2015**, *113*, 46−56.

(41) Vandeputte, A. G.; Reyniers, M.-F.; Marin, G. B. *Theor. Chem. Acc.* **2009**, *123*, 391−412.

(42) Vandeputte, A. G.; Reyniers, M.-F.; Marin, G. B. *J. Phys. Chem. A* **2010**, *114*, 10531−10549.

(43) Vandeputte, A. G.; Sabbe, K. M.; Reyniers, M.-F.; Marin, G. B. *Phys. Chem. Chem. Phys.* **2012**, *14*, 12773−12793.

(44) Vandeputte, A. G.; Reyniers, M.-F.; Marin, G. B. *ChemPhysChem* **2013**, *14*, 1703−1722.

(45) Vandeputte, A. G.; Reyniers, M.-F.; Marin, G. B. *ChemPhysChem* **2013**, *14*, 3751−3771.

(46) Arican, H.; Arthur, N. L. *Aust. J. Chem.* **1983**, *36*, 2195.

(47) Perrin, D.; Richard, C.; Martin, R. *J. Chim. Phys.* **1988**, *85*, 185.

(48) Zeng, Z.; Altarawneh, M.; Oluwoye, I.; Glarborg, P.; Dlugogorski, B. *J. Phys. Chem. A* **2016**, *120*, 8941−8948.

(49) Balla, R. J.; Nelson, H. H.; McDonald, J. R. *Chem. Phys.* **1986**, *109*, 101.

(50) Tyndall, G. S.; Ravishankara, A. R. *J. Phys. Chem.* **1989**, *93*, 2426.

(51) Zhu, L.; Bozzelli, J. W. *J. Mol. Struct.: THEOCHEM* **2005**, *728*, 147−157.

(52) Turnipseed, A. A.; Barone, S. B.; Ravishankara, A. R. *J. Phys. Chem.* **1992**, *96*, 7502−7505.

(53) Gersen, S.; Mokhov, A. V.; Darmeveil, J. H.; Levinsky, H. B. *Combust. Flame* **2010**, *157*, 240−245.

(54) Gersen, S.; Mokhov, A. V.; Darmeveil, J. H.; Levinsky, H. B.; Glarborg, P. *Proc. Combust. Inst.* **2011**, *33*, 433−440.

(55) Lee, D.; Hochgreb, S. *Combust. Flame* **1998**, *114*, 531−545.

(56) Lutz, A. E.; Kee, R. J.; Miller, J. A. *SENKIN: A Fortran Program for Predicting Homogeneous Gas Phase Chemical Kinetics with Sensitivity Analysis*; Sandia National Laboratories: Livermore, CA, 1987; Sandia Report SAND87-8248.

(57) Rasmussen, L.; Hansen, J.; Marshall, P.; Glarborg, P. *Int. J. Chem. Kinet.* **2008**, *40*, 454−480.